# Text Recognition - Real World Data and Where to Find Them

Klara Janouskova, Jiri Matas Centre for Machine Perception, Department of Cybernetics Czech Technical University, Prague, Czech Republic Lluis Gomez, Dimosthenis Karatzas Computer Vision Center Universitat Autonoma de Barcelona, Spain

Abstract—We present a method for exploiting weakly annotated images to improve text extraction pipelines. The approach exploits an arbitrary existing end-to-end text recognition system to obtain text region proposals and their, possibly erroneous, transcriptions. A process that includes imprecise transcription to annotation matching and edit distance guided neighbourhood search produces nearly error-free, localised instances of scene text, which we treat as "pseudo ground truth" used for training.

We apply the method to two weakly-annotated datasets and show that the process consistently improves the accuracy of a state of the art recognition model across different benchmark datasets (image domains) as well as providing a significant performance boost on the same dataset.

#### I. INTRODUCTION

Written text is an important source of information for humans and plays an important role in everyday life, being a frequent part of scenes with man-made structures. It is one of the most common classes in general object detection datasets like CoCo [1]. Research in end-to-end reading systems is a very active field attracting the attention of both researchers and companies. It is an essential part of many applications ranging from translation systems and autonomous driving to image retrieval or visual question answering.

In recent years, with the introduction of deep neural network models, the field has advanced substantially. At the same time, state of the art performance comes at the cost of the requirement of large-scale annotated data for training. Such data need to be rich in geometry, style and content. Typical ground truth data is defined at the granularity of words as polygonal regions in the image along with the corresponding text transcriptions. The acquisition of such data requires substantial human effort and is very costly.

The lack of data is usually approached in two different ways, either by generating synthetic data as in [2], [3], [4], [5], [6], [7] or with different forms of weakly, semi or unsupervised learning on real data as in [8], [9], [10].

While fully annotated real world data are expensive and sparse, weakly annotated data in the form of images along with a set of words likely to appear in them are common. An example of a source for such weakly annotated data are product databases where we can readily obtain the name of the product and other meta-data. Illustration of a weakly annotated dataset, based on a product database, used in our experiments is shown in Figure 1. Images from mapping services like Google Maps are another potential source where street names

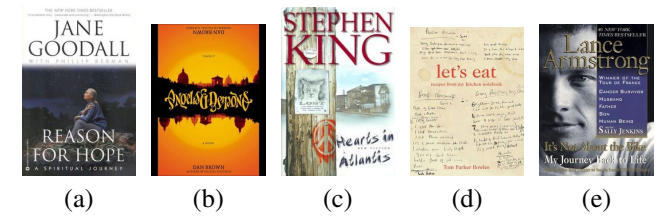


Fig. 1: The ABC Dataset images are diverse, some have (a) both a simple layout and font, (b) a very artistic, almost illegible font and (c) a font that resembles handwriting. Other have (d) both dense background and hand-written text or (e) the background varies significantly even at the word level. The dataset includes weak annotations - the name of the author and the title. Not all text is annotated, location of the annotated text is not provided.

and numbers or business names are words very likely to appear in an image and easily obtainable through location-based search. For example, given images from the location where a restaurant is supposed to be, it is expected that the name of the restaurant will be visible in some of them.

In this paper, we present a new method for automatically generating pseudo ground truth (PGT) in the form of text regions and their transcription from weakly annotated data consisting of text transcriptions only with no information about the text location. The method requires an end-to-end text recognition system (E2E) pre-trained with another source of annotated data. To our knowledge, previous methods for weakly supervised learning used weak labels which alleviate but do not eliminate human participation, such as annotating only the areas of interest or localizing words instead of characters.

The core idea is that the OCR output of the recognition model can be used to identify the most probable text match from the weak annotations by finding the one with the lowest edit distance. The detections that produce an exact match with the weak label are assumed to be correct. Furthermore, the recognition output can be used to find the modifications of the detected regions that minimize the edit distance to the matched text. For example, if we have predicted the word 'car' and the best match was 'cartoon', running the recognition again on the detected region extended to the right may decrease the distance between the matched and predicted text, possibly leading to

the prediction of the matched word 'cartoon'. The probability of the recognition model giving the same output as the weak label for a wrong text region is very low, thus it is safe to use such regions as PGT for further training.

In summary, given an image and a dictionary of words as an input, the method outputs a subset of the dictionary words with their corresponding text regions in the image. The method is independent of the underlying implementation of the models used and is able to handle incomplete (not all the text in the image is in the dictionary) and noisy (the dictionary contains words that are not present in the image) labels.

Possible applications of our method are improving the performance of an existing general E2E system or domain adaptation, where the source domain has full ground truth data available whereas only weak labels are available for the target domain.

We apply our method to data from two different sources - a database of images of book-covers downloaded from Amazon books, using the title and the author of the book as weak annotations, and the Uber-Text dataset [11], which is very similar to the kind of data that could be obtained using a mapping system. We train a recognition model with the PGT generated from both sources on various benchmarks, showing that it consistently improves the recognition accuracy across a wide range of datasets. While the images from the Uber-Text dataset are annotated and applying our method to them does not produce additional value in terms of generated PGT, working with a large-scale annotated dataset allows us to compare the performance of our method to fully supervised training, showing its applicability for domain adaptation. The accuracy of the method is analyzed..

The contributions of the paper are:

- A new method for automatically generating pseudo ground truth data from images with weak annotations.
- We show that a state of the art model trained with the PGT generated from two different sources performs well on a wide range of benchmark datasets, the accuracy is consistently boosted even when the PGT data originates from a very different distribution.
- The PGT method improves significantly recognition performance in weakly-supervised domain adaptation.
- The localization of the PGT texts in the Amazon Book Covers dataset will be made public.

# II. RELATED WORK

We first give a short introduction of scene text detection and recognition methods, and an overview of methods for generating synthetic data. Then we focus on weakly-supervised learning for text detection and recognition.

# A. Text Detection and Recognition

Before the deep learning era, methods based on SWT or MSERs were used for text detection, for example [12], [13]. Subsequent models were mostly based on region proposal approaches like [14]. Recently, methods have rather turned

to segmentation-based approaches like [15] and focused on representing arbitrarily shaped text, for example [8], [16].

Recent approaches for text recognition rely on deep learning. Most methods can be described by 4 stages. Transformation - a Spatial Transformer Network [17] normalizing the input image. Feature extraction - a CNN such as VGG [18] or ResNet [19] maps the input image to feature maps. Sequence modelling - BiLSTMs are used to provide contextual information to the feature maps. Prediction - either CTC [20] or attention-based prediction [21] is used to convert the encoded features into a character sequence. Some methods treat the two tasks jointly, sharing features for both detection and recognition, for example [22], [23], [24].

# B. Synthetic data for text detection and recognition

The work of [5] and [14] had a great influence on the performance of text detection and recognition systems. Synthetic data have proven to be very effective for training generic text localisation systems. Still, the lack of realism (both in terms of positioning, and blending with the scene), diversity (in terms of text styles and scene backgrounds) and contextualisation of the text in the scene, have been limiting factors. More recent works aim to improve some of these aspects [2], [4], [6], [7], or exploit instead real scene text data to do augmentation [3], still, cannot replace the quality of real-world data.

# C. Weakly Supervised Learning for Text Detection and Recognition

The proposed method builds on top of pseudo-labelling techniques [25], a simple strategy for semi-supervised learning where part of the data is fully labelled and Pseudo-Labels are created for unlabelled data as the class with the maximum predicted probability and further treated as true labels.

In [26], focused on Chinese street view images, weak annotations are used where only the text-of-interest region is annotated. They suggest an online proposal matching module incorporated in the whole model. The main difference from our method is that they do not do any modification of the proposed regions.

In [24], an existing OCR engine different from the one being trained is used to provide partial labels for one million unlabelled images. The partially labelled data is then used to train the recognition part of an E2E model, improving the results significantly. The method relies on a confidence threshold to filter out noisy labels while our method relies on weak annotations to minimize the risk of incorrect labelling.

Focusing on text detection, [10] propose multiple approaches for unsupervised and weakly supervised learning. Their unsupervised approach simply relies on filtering out predictions with low confidence score. An improved approach requires weak annotations, where regions containing text are annotated and it is known that regions distant from the annotated ones do not contain any text, allowing for more accurate false positives filtering. Their last approach relies on rectangular bounding boxes as weak labels.

#### III. DATASETS

In this section, we introduce the datasets used for training, evaluation and PGT generation.

**Amazon Book Covers (ABC)** is a dataset created from more than 200,000 images downloaded from Amazon Books. The author and the title of each book serve as weak annotations. The same data were already used for genre prediction in [27]. Some illustration images are shown in Figure 1.

**Uber-Text dataset (UT)** is one of the biggest datasets for text detection and recognition. It contains 117,969 images with 571,534 labelled text instances split into training, validation and test sets. Each set is divided into two subsets according to the image resolution - either 1K or 4K. The images were obtained through the Bing Maps Streetside program and come from 6 different cities in the US. The annotations are line-level. Most of the text regions form semantic units such as business names, street signs or street numbers. The datasets contains a lot of unannotated text, some text regions are not annotated at all, some readable text is labeled as unreadable [11].

**MJSynth (MJ)** contains almost 9M synthetically generated images of English words for text recognition. The text generation process performs the following steps: Font rendering, border/shadow rendering, coloring, projective distortion, natural data blending and noise introduction [14].

**SynthText (ST)** is a synthetic dataset designed for scenetext detection, widely used for recognition, too. It has over 7M text instances in 8,000 images [5].

Synthetic Multi-Language in Natural Scene Dataset (MLT) contains 245,000 images in total with text instances in multiple scripts: Arabic, Bangla, Chinese, Japanese, Korean and Latin. The dataset was published in [23] and the authors have adapted the framework of [5]. A non-latin dictionary was used and it contains special, non-alpha-numeric characters. We only use the Latin script subset of the dataset, which contains 288,917 text instances in total [23].

**IIIT 5K-word (IIIT)** is a collection of 5,000 cropped words from Google image search using queries such as 'billboards' or 'movie posters', which are likely to contain text [28]. The training set consists of 2,000 images, the remaining 3,000 form the test set.

**Street View Text (SVT)** was collected from the Google Street View, providing annotators with a lexicon for each image, containing texts such as business names. Only the words from the lexicon were localised and provided with transcription, the rest of the text is ignored. There are 257 and 647 images of cropped words in the training and test sets [29].

**Street View Text - Perspective (SVT-P)** is a dataset of 645 images collected from Google Street View focused on perspective projections [30].

**ICDAR2003** (**IC03**) has 258 training and 251 testing images with 1,156 and 1,110 annotated words respectively. It was collected for the ICDAR 2003 Robust Reading competitions [31].

ICDAR2013 (IC13) is a dataset with 'focused text', the text being the main content of the image. It consists of a training

set of 229 image with 848 words and a test set of 233 images with 1095 words. [32].

**ICDAR2015** (**IC15**), in contrast to IC13, focuses on incidental scene-text - the images were not taken with text in mind. The training set contains 1000 images (4,468 words) and the test contains 500 images (2,077 words) [33].

**Total-Text** (**TT**) is a dataset of 1,555 scene images with 9,330 annotated words. The images were collected with curved text in mind and the images often contain texts of different orientations [[34]].

**CUTE80** (**CT**) contains 80 images with 288 words, focusing on curved text [35].

# IV. PGT GENERATION

This section describes the pseudo ground truth (PGT) generation algorithm (PGT-GEN). The algorithm uses weakly annotated images and an existing end-to-end reading system (E2E). All the steps are executed independently for each image. First, we define the E2E output and the structure of the weak annotations. Then we describe the algorithm and its components in detail.

Given an image I, the output  $O = \{(bb_1, tt_1), \dots (bb_t, tt_t)\}$  of the end-to-end reading system is a set of t text bounding box predictions and the corresponding text transcriptions. The transcriptions  $T = (tt_1, \dots, tt_t)$  are strings (possibly containing spaces) and the bounding boxes are oriented rectangles. It is necessary that the recognition output from a bounding box bb can be obtained independently: REC(I, bb) = tt.

Each image is associated with a list of texts  $A=(t_1,t_2\dots t_n)$  where each text  $t_i=(w_1,w_2,\dots,w_m)$  is a non-empty ordered sequence of words. The set of weak labels  $G=\bigcup_{i=1}^n g_i$  is obtained as a union of sets of k-grams,  $k\in\{1,..5\}$ . Each set of k-grams  $g_i$  is formed by strings (consecutive words from  $t_i$ ), sub-sequences of  $t_i$  of length k joined into a single string by the space character. In the simplest of cases, each text  $t_i$  only consists of a single word but because the texts are assumed to be extracted automatically as metadata accompanying the images, it may even be multiple words that form a semantic unit — a name of a product, its description, a business' name, contact information. These words are likely to appear in the image close to each other and get merged by the detector.

For example, an image could be annotated with the texts "Sherlock Holmes" and "221B Baker Street". In that case,  ${\cal A}$  and  ${\cal G}$  would be

```
A = ((\text{``Sherlock''}, \text{``Holmes''}), (\text{``221B''}, \text{``Baker''}, \text{``Street''})) G = \{\text{``Sherlock''}, \text{``Holmes''}, \text{``Sherlock Holmes''}, \text{``221B''}, \text{``Baker''}, \text{``Street''}, \text{``221B Baker''}, \text{``Baker Street''}\}.
```

# A. PGT-GEN algorithm

The PGT-GEN algorithm takes the image I, E2E output O and the set of weak labels represented as k-grams G as an input and outputs the PGT - a localized subset of G.

# 

**AssignWeak - Weak annotation assignment.** Each element from O is assigned at most one weak annotation from G. We construct a directed bipartite graph  $B_G = (V, E)$  between O and G, thus  $V = O \cup G$ . For each output  $o \in O$ , o = (bb, tt) and weak annotation  $g \in G$  it holds that

$$(o,g) \in E \iff \operatorname{dist}(tt,g) = \min_{i=1}^{|G|} \operatorname{dist}(tt,g_i) \qquad (1)$$

$$(g,o) \in E \iff \operatorname{dist}(tt,g) = \min_{i=1}^{|T|} \operatorname{dist}(tt_i,g)$$
 (2)

where dist is the Levenshtein distance.

Then, a set of proposals P is created:

$$P = \bigcup_{i=1}^{|O|} \operatorname{Assign}(o_i, E) \tag{3}$$

$$\operatorname{Assign}(o,E) = \begin{cases} \emptyset & \text{for } W(o,E) = \emptyset \\ [W(o,E)]_R & \text{otherwise} \end{cases} \tag{4}$$

$$W(o, E) = \{(o, g) : (o, g) \in E \land (g, o) \in E \land \mathsf{match}(o, g)\}.$$

We define  $\operatorname{match}((bb,tt),g) = \frac{\operatorname{dist}(tt,g)}{\operatorname{max}(\operatorname{len}(tt),\operatorname{len}(g))} < 1$  to filter out completely irrelevant proposals and  $[.]_R$  selects an element from a set randomly. In most cases,  $|W(o,E)| \in \{0,1\}$ .

At this point, we could apply some simple filtering to the set of proposals P instead of the edit distance guided neighbourhood search, for example, select

$$P' = \{ p \in P, p = ((bb, tt), g) | dist(tt, g) = 0 \}$$
 (6)

and then output

$$PGT = \bigcup_{((bb,tt),g)\in P'} (bb,tt). \tag{7}$$

This would be equivalent to selecting such proposals where the predicted transcription was equivalent to the weak label text for PGT - we implement this version and compare it to the proposed one, showing the superiority of the proposed method.

FindOptimalBox - Edit distance guided neighbourhood search. For each proposal  $((bb, tt), g) \in P$ , we search for an



Fig. 2: Improved localization of weak labels by the neighbourhood search - the detected bounding boxes (blue) and the transformed ones (green).

optimal bounding box  $bb_f$  which minimizes the Levenshtein distance between the recognized text  $tt_f$  and g.

If  $\operatorname{dist}(tt,g)=0$ , we assume that bb is already optimal and assign  $bb_f=bb$ . If not, we predefine a set of new boxes in the neighbourhood of bb and run the recognition on those in parallel, selecting one with minimal distance from g for  $bb_f$ . The generation of the set of predefined boxes is explained in detail in Appendix A.

We compute  $tt_f = \text{REC}(I, bb_f)$  and the normalized edit distance between  $tt_f$  and g as  $d = \frac{\text{dist}(tt_f, g)}{\max(\text{len}(tt_f), \text{len}(g))}$ .

Finally, we find out whether  $(bb_f,tt_f)$  satisfies our requirements for being a PGT (IsPGT) as:

$$\text{IsPGT}(tt_f,g) = \begin{cases} True & \text{for } d = 0 \lor \text{isClose}(d,tt_f,g) \\ False & \text{otherwise} \end{cases}$$

where  $\operatorname{isClose}(d,tt_f,g)=(d<\theta \wedge |tt_f|>\lambda \wedge tt_f^0=g^0 \wedge tt_f^{-1}=g^{-1}),\ s^0,s^{-1}$  are the first and the last characters of a string s. The thresholds  $\theta,\ \lambda$  are set to  $\theta=0.35,\lambda=4$ . The intuition behind the IsClose function is that even if the recognized text  $tt_f$  and the assigned text g are not identical, it is possible that there was simply an error in the recognition step. If the relative edit distance between two longer texts is low and the first and the last characters are the same, it is likely that  $tt_f$  should actually be g.

Examples of how the neighbourhood search aids the PGT generation process can be seen in Figure 2.

# V. END-TO-END READING SYSTEM

In this section, the end-to-end reading system (E2E) used in our experiments is described. Separate models for detection and recognition are used.

# A. Detection

For text detection, we adopt TextSnake [16]. It is based on a fully convolutional network – U-net with VGG-16 [18] backbone – which estimates the geometry attributes of text instances. A text instance is described as a sequence of ordered, overlapping disks centered at symmetric axes, each of which is associated with potentially variable radius and orientation.

The following values are predicted for each pixel: tcl, tr, r and  $\alpha$ , corresponding to the text center line, text region, radius and angle. Thresholds varying on different datasets are applied to tcl and tr to obtain binary masks  $tcl_b$  and  $tr_b$ . Focusing on straight text, we replace the proposed subsequent post-processing steps for text instance reconstruction with a method

based on least squares fitting of the text center line points, which improves the orientation of the final bounding box.

First we obtain the connected components CC from  $tr_b*tcl_b$ . For each component  $cc \in CC$ , where cc are all the component points, we estimate the bounding box  $(c_x, c_y, w, h, \alpha)$  directly.

The angle  $\alpha$  is estimated by total least squares fitting of a line to the points of cc shifted by the mean value of the coordinates  $m=(m_x,m_y)$  to the origin, using the slope of the best fitting line as the bounding box angle.

The height h is determined via the biggest radius predicted within the component: h=max(r[cc])\*2. To determine the width w, we project the shifted points onto the line with slope  $\alpha$  passing through the origin and find the projected vectors with maximum norm in both directions,  $p_{pos}$  and  $p_{neg}$ . The width is calculated as  $w=|p_{pos}-p_{neg}|+h$ . The extra h is added to the width because during training, the tcl is shrank by  $\frac{h}{2}$  (assuming the radius is constant,  $\frac{h}{2}$ , for straight text with rectangular ground truth). Afterwards, we shift  $p_{pos}, p_{neg}$  back by m and calculate the center of the bounding box as the middle point:  $(c_x, c_y) = m + \frac{p_{pos} + p_{neg}}{2}$ .

#### B. Recognition

We adopt the best performing architecture from [36], which is very similar to the one of STAR-net [37] but with different prediction mechanism.

1) Transformation: The transformation module transforms an input image I into a rectified image  $\tilde{I}$ . It predicts the parameters of a thin-plate spline (TPS) transformation, a variant of spatial transformer network (STN) [17]. The whole module consists of a localization network, a grid generator and a grid sampler.

We use grayscale images as the input and both the input and output dimension are fixed to  $32 \times 150$  pixels. For more details, we refer the reader to [38], [36], [37].

2) Feature Extraction: Given the rectified image  $\tilde{I}$ , the feature extractor outputs a feature map

$$V = \text{CNN}(\tilde{I}) = \{v_i\}, i = 1, \dots K$$

$$(9)$$

where K=38 is the number of columns in the output feature map  $(512 \times 38)$ .

- 3) Sequence modeling: a BiLSTM network [39] creates contextual features from the visual features  $v_i$  and outputs  $H = \mathrm{Seq}(V)$ . We use a 2-layer BiLSTM. An  $i^{th}$  layer identifies two hidden states: forward  $h_i^{(t),b} \forall t$ . A fully-connected layer between the two BiLSTM layers determines one hidden state,  $\hat{h}_t^{(i)}$ , from  $h_i^{(t),f}$  and  $h_i^{(t),b}$ . The dimension of the hidden states and the FC layer is 256.
- 4) Prediction: Finally, a single layer LSTM [40] attention decoder produces the output sequence of characters  $Y = y_1, y_2, \ldots y_n$ ,  $y_t = \operatorname{softmax}(W_o s_t + b_o)$ , where  $W_o$  and  $b_0$  are trainable parameters, and  $s_t$  is the decoder LSTM hidden state at time t. The decoding stops when the (EOS) symbol is emitted. The model is trained with the cross entropy loss function. For more details on the attention mechanism, please see [8], [21], [24].

This recognition model is used in all of our experiments and we will refer to it simply as OCR.

# VI. EXPERIMENTS

The pseudo ground truth (PGT) generation method was tested with two different sources of weakly annotated data, the Amazon book covers dataset (ABC) and the Uber-Text (UT) training set where we ignored line-level localization information.

The detection part of E2E (TextSnake) was trained on a mix of SynthText, ICDAR2015 and Total-Text datasets. The post-processing thresholds of TextSnake were set to tr=0.4 and tcl=0.7, which lead to the best PGT generation performance on a small subset of UT and ABC images. We do not filter out the text marked as unreadable or don't care during training to maximize the use of available data. Detection recall is more important than precision for PGT generation—the more words detected, the more potential pseudo-labelled examples are available. On the other hand, false positives are very unlikely to be matched against weak annotations, thus they have minimal impact, besides slowing down the process.

The recognition part (OCR), which also serves as a baseline model (OCR $_b$ ) in our experiments, was trained on the ST (Synth-text), MJ (MjSynth) and MLT (Synthetic Multi-Language in Natural Scene) datasets. The OCR $_b$  recognizes 70 characters – letters, not distinguishing lower and upper case, digits and frequent special characters like punctuation, brackets, the (EOS) symbol and the space.

Most recognition datasets provide word-level annotations, and thus space is never part of the transcription. We included space in the character set for three different reasons. First, if the model is capable of predicting spaces, it helps to guide the PGT generation process - a bounding box that is too wide leads to a space being predicted at the beginning or end of the transcription. Second, if the detector merges horizontally adjacent words into a single bounding box, the recognizer often splits the text by recognizing a space between the merged words. Third, it allows exploiting annotations that contain multiple words.

Synthetic datasets used for training have word-level annotations and thus provide no training data for the space character. We therefore extended some of the bounding-boxes and included spaces at the beginning and end of the ground truth annotations. This produced a model with a limited ability to recognize the space. The ability was further improved during training on PGT, since it contains multi-word texts. During evaluation, we strip any leading/trailing spaces from the predictions.

The OCR processes images with a fixed resolution of  $32 \times 150$ . Input images are first resized isotropically to height 32. If the width of the resized image is less than 150, the image is extended to the left and padded with zeros. If the width exceeds 150, the image is horizontally shrunk to 150 only in this case the aspect ratio of the input images is not preserved.

Iteration #	Mined with n. s.	Mined w/o n. s.	$\Delta$
1	92,909	72,990	19,919
2	105,126	86,295	18,831
3	109,557	90,480	19,077
4	111,663	92,660	19,003
5	113,046	93,994	19,052
6	113,810	94,890	18,920

TABLE I: PGT generation on the Uber-Text training dataset where text location information is ignored. The number of captions generated in iterations 1 to 6, with and without the neighbourhood search, and the difference  $\Delta$ .

# A. PGT from the Uber-Text dataset

The experiment evaluates the PGT method as an adaptation technique to the Uber-Text dataset domain. The performance is also compared to fully supervised training in the UT domain.

A reference method,  $OCR_{UT_F}$ , is obtained by fully supervised training on  $UT_F$ , the set of 138,437 transcriptions and corresponding rectangular crops from the UT training set that contain no unreadable characters in transcription. The crops are the minimum area enclosing rectangles of the ground truth polygons.  $OCR_{UT_F}$ , as well as other OCRs described in this section, are validated on a set of 5,000 random transcriptions from the UT validation set is created.

For PGT generation, the whole UT training set is used. To facilitate GPU computations, we split large (about 4K) images into 16 blocks ensuring no text instance is split and discard those with no text. Such empty blocks are common, since text instances are sparse in many images. Each of the original ground truth transcriptions is a weak label in our experiment, the ground truth polygons are discarded. The weak labels are transformed into a set of n-grams, as explained in the PGT generation section. N-grams containing the \* symbol (unreadable or unknown characters) are discarded.

The PGT generation and OCR training progresses iteratively. First, the  $OCR_b$  results are processed, creating the  $UT_1$  PGT dataset. Next, an updated model,  $OCR_{UT_1}$ , is trained with  $UT_1$ . In the k-th iteration, k>1, while keeping the detections fixed, the OCR trained in the previous iteration,  $OCR_{UT_{k-1}}$ , generates the new  $UT_k$  dataset.

*PGT generation and OCR training.* In the first iteration, 92,909 PGT text instances were obtained. The number of PGT texts increased in all iterations, reaching 113,810 texts after six iterations when the OCR performance stopped improving – a summary is shown in Table I. The recognition rate, calculated on 20 000 randomly selected transcriptions from the UT test set, increased in each iteration from the baseline 41.6 % to 66.1 % in the sixth iteration. The accuracy of the fully supervised  $OCR_{UT_F}$  is 78 %. The PGT has reduced the gap between the baseline model and the fully-supervised one by 67 %. The performance of PGT training is limited by the detector which was not trained on the new domain. Improving the detector may help to reduce the gap further.

To test the contribution of the neighbourhood search and of allowing imperfect matches, a dataset, denoted  $UT'_1$ , is created. It contains only the detections that matched with 0

	7	Training	g dataset:	ple %			
			Full		Weak		
	MJ	ST	MLT	UT <sub>F</sub>	UT (30)	Acc.	Norm. ED
[11]						56.4	
$OCR_b$	45	45	10	0	-	41.6	35.2
$OCR_{UT'_1}$	30	30	10	0	$\mathrm{UT}_1'$	55.2	28.0
OCR <sub>UT</sub> 1	30	30	10	0	$UT_1$	57.9	26.2
$OCR_{UT_2}$	30	30	10	0	$\mathrm{UT}_2$	62.7	23.3
OCR <sub>UT</sub> 2	30	30	10	0	$UT_3$	64.4	22.5
$OCR_{UT_4}$	30	30	10	0	$\mathrm{UT}_4$	65.4	21.5
$OCR_{UT_5}$	30	30	10	0	$UT_5$	66.0	21.1
$OCR_{UT_6}$	30	30	10	0	$UT_6$	66.1	21.2
${{ m OCR}_{{ m UT}_6}} \ {{ m OCR}_{{ m UT}_F}}$	30	30	10	30	-	78.0	10.0

TABLE II: Recognition rates (acc.) on the Uber-Text test set. The data obtained from the  $i^{th}$  iteration of the PGT generation is denoted as  $UT_i$ .  $UT_F$  is the fully annotated dataset and  $UT_1'$  is a subset of  $UT_1$  obtained without the neighbourhood search.

edit distance with some of the weak labels. The accuracy of the model trained with  $UT_1'$  is 2.7 % lower, showing the importance of the additional retrieved PGT text. Table II summarizes the UT experiments.

# B. PGT from book covers

Iteration / Mined:	total	w/o neigh. s.	with neigh. s.
1	1,536,583	1,234,219	302,364
2	1,581,109	1,354,219	226,890
3	1,594,333	1,375,571	218,762

TABLE III: Pseudo-ground truth (PGT) generation performance on the ABC dataset. The number of boxes with text generated: in total, without and with the neighbourhood search.

The PGT is generated from the whole ABC dataset - over 200,000 images, using the author and the title of each book as weak label. The title often includes a subtitle - while the author and title are almost always present in the image, the subtitle is less common, or there may only be a part of it.

We performed three iterations, in the first, the  $OCR_b$  model generates the  $ABC_1$  PGT dataset of 1,536,583 cropped images of texts. The model trained with this data is referred to as  $OCR_{ABC_1}$ . In the second iteration, using  $OCR_{ABC_1}$  instead of  $OCR_b$ , we obtain the  $ABC_2$  dataset with 1,581,109 images. Finally, the  $OCR_{ABC_2}$  model is trained and used to generate  $ABC_3$ , a dataset of 1,594,333 images. A summary of the PGT generation results from all the iterations can be found in Table III.

# C. PGT accuracy

We have analyzed the accuracy of the PGT method on a subset of  $UT_6$  and  $ABC_3$  - 500 samples from each dataset. The frequencies of different kind of errors are reported in Table IV - PGTs with image that does not contain text, PGTs where the label is wrong, PGTs that contain an error in punctuation and PGTs where the error is due to a wrong weak label. A more detailed analysis can be found in Appendix B. Note that the majority of the 'not text' and 'wrong label' are due to false positives/very blurred texts, leading to a prediction of a common word such as 'the', 'on', 'in' with a low confidence and thus can be filtered out easily.

	ABC	UT
not text	1	2
wrong label	19	6
punctuation	1	2
weak label error	0	7

TABLE IV: The frequencies of different kind of errors on a subset of  $ABC_3$  and  $UT_6$  - 500 samples from each.

#### D. Results on benchmark datasets

A recognition model trained with the PGT data from the previous experiments is evaluated on different domains using various commonly used recognition datasets - IIIT 5K-word (IIIT), Street View Text (SVT), ICDAR2003 (IC03), ICDAR2013 (IC13), ICDAR2015 (IC15), Street View Text - Perspective (SVT-P) and CUTE80 (CT). We evaluate on test set subsets commonly used by researches as identified in [36]. All the models were validated on a union of the training sets of all the previously mentioned datasets. The reported metric is the percentage of correctly recognized words.

To evaluate models trained on word-level data only, a test set of 20,000 images where each image only contains a single word, referred to as  $UT_W$ , is also created.

We also evaluate on the  $UT_W$  subset of the UT dataset but it was not included in the validation set. We remove any spaces from all the predictions and when evaluating on datasets with images that contain punctuation but the ground truth does not, we filter any non-alphanumeric characters out.

Training with either  $UT_1$  or  $ABC_1$  generated in the first iterations of the PGT generation consistently improves the performance. For some datasets, UT boosts the performance more than ABC and vice versa and training with both leads to a superior performance on all evaluated datasets. Training with the data from the last iterations,  $UT_6$  and  $ABC_3$ , further improves the accuracy with an average improvement of 3.7 % relative to  $OCR_b$ .

The model trained with the  $UT_1'$  and  $ABC_1'$  datasets is also evaluated. Those datasets are subsets of the  $UT_1$  and  $ABC_1$  datasets that would have been obtained if no neighbourhood search or edit distance filtering was used. With the exception of IC03 dataset, this model's performance is always inferior to the model trained with all the data.

The results also show that while the baseline model trained on synthetic data only performs well over a wide range of different datasets, the performance on UT dataset is rather poor - only 52.8 % accuracy. This shows the challenging nature of the dataset, which is partially due to the presence of heavily blurred images and the high frequency of vertical/diagonal text direction.

The summary of the experiments can be seen in Table V.

For better comparison with other methods, we also trained and evaluated our best performing model on alpha-numeric characters only. The baseline model is pretrained with MJ and ST and fine-tuned with the UT<sub>6</sub> and ABC<sub>3</sub>. During evaluation, all images with unknown characters are filtered out. The boost in performance here is slightly lower, 3.3 % on average.



Fig. 3: Images with improved results after PGT training. The original  $OCR_b$  and  $OCR_{UT_6+ABC_3}$  ( $\rightarrow$ ) predictions.



Fig. 4: Images with worse results after PGT training. The original OCR<sub>b</sub> and OCR<sub>UT<sub>6</sub>+ABC<sub>3</sub></sub> ( $\rightarrow$ ) predictions.

As far as the authors are concerned, the recognition model [36] used in our experiments is the best performing architecture with publicly available code-base. While the performance of our retrained model does not surpass that of overall state-of-the-art models, the results clearly show that training with automatically generated pseudo ground truth can significantly increase the accuracy. Not only can the same data be used to retrain the model but if a model with a better architecture is used to generate the PGT, the amount of PGT is likely going to increase, possibly leading to better results than with our version of PGT. It is important to realize that all the improvements reported in this paper were achieved with no changes to the network architecture.

The results of our work show that training with automatically generated PGT from very different domains, such as born-digital documents, can significantly improve the performance of a recognition model over a wide range of scenetext datasets. Also, adding only a relatively small number of those images helps significantly, implying the variety of data is important. Some common characteristics of the images where the PGT data has improved the model's performance are blurred images, perspective distortions, artistic/handwritten fonts or occluded/cropped characters. Examples are shown in Figure 3 while images where the performance has deteriorated are shown in Figure 4.

#### VII. CONCLUSION

We proposed a PGT generation method and applied it to two different sources of weak annotations. Traning with PGT

	Tra	ining	dataset -	examp	ole %	Evaluation on							5	Summai	·y		
		Full		W	Weak		SVT	IC03	IC13	IC15	SP	CT		Δ		$UT_{w}$	Δ
	MJ	ST	MLT	UT	ABC	3000	647	867	1015	2077	645	288	avg	min	max	20 000	
$OCR_b$	45	45	10	0	0	89.8	86.7	94.3	91.2	68.5	77.2	72.3	0.0	0.0	0.0	52.8	0.0
OCR <sub>ABC</sub> <sub>1</sub>	30	30	10	0	30	92.8	88.9	94.8	93.0	71.0	77.5	73.6	1.7	0.3	3.0	53.9	1.1
OCR <sub>UT1</sub>	30	30	10	30	0	92.2	88.6	95.0	94.1	70.6	79.2	76.4	2.3	0.7	4.1	61.6	8.8
OCR <sub>UT1+ABC1</sub>	20	20	10	20	30	93.0	89.2	95.2	94.1	71.6	79.2	77.8	2.9	0.9	5.5	61.8	9.0
OCR <sub>UT6</sub> +ABC <sub>3</sub>	20	20	10	20	30	93.5	90.7	95.5	94.0	74.6	80.1	77.8	3.7	1.2	6.1	67.8	15.0
OCR <sub>UT'</sub> +ABC'	20	20	10	20	30	91.4	88.1	95.5	93.9	69.5	77.1	74.0	1.4	-0.1	2.7	59.1	6.3

TABLE V: Recognition rate on standard benchmarks, non-alphanumeric characters included. Validation was performed on the union of training sets, with the exception of the UT dataset. Average, min. and max. improvements relative to  $OCR_b$  ( $\Delta$ ).  $UT_w$  results are not added to the summary since PGT was extracted from the UT domain and higher improvements are observed.

	Trair	ing da	itaset - 6	example %	Evaluation on							Summary				
	Fı	ıll	1	Weak	IIIT	SVT	IC03	IC13	IC15	SP	CT		Δ		UTw	Δ
	MJ	ST	UT <sub>6</sub>	ABC <sub>3</sub>	3000	647	867	1015	1922	645	287	avg	min	max	18 956	
$OCR_b$	50	50	0	0	87.6	88.6	94.5	91.9	75.2	78.9	73.2	0	0	0	54.9	0.0
OCR <sub>UT6</sub> +ABC <sub>3</sub>	25	25	20	30	91.7	91.8	95.7	94.2	80.0	82.5	77.4	3.3	1.2	4.8	68.9	14.0
Published SOTA	†	†	†	†	95.3	92.7	96.6	96.4	82.8	87.0	88.5					
References					[15]	[41]	[41]	[42], [15]	[41]	[41]	[15]					

TABLE VI: Recognition rate on standard benchmarks excluding images containing non-alphanumeric characters. Like many published methods, the model was pre-trained with MJ and ST datasets. Average, min. and max. increment relative to OCR<sub>b</sub> ( $\Delta$ ). †Published SOTA methods were each trained on different datasets.

consistently improved the accuracy of a state of the art model both on images from the same domain and across different benchmark datasets and thus different domains.

#### REFERENCES

- [1] Veit et al., "Coco-text: Dataset and benchmark for text detection and recognition in natural images," arXiv:1601.07140, 2016.
- [2] Chen et al., "Cross-domain scene text detection via pixel and imagelevel adaptation," in NIPS. Springer, 2019, pp. 135–143.
- [3] R. Gomez et al., "Selective style transfer for text," in ICDAR, 2019, pp. 805–812.
- [4] Zhan *et al.*, "Ga-dan: Geometry-aware domain adaptation network for scene text detection and recognition," in *ICCV*, 2019, pp. 9105–9115.
- [5] Gupta et al., "Synthetic data for text localisation in natural images," in CVPR, 2016, pp. 2315–2324.
- [6] Liao et al., "Synthext3d: Synthesizing scene text images from 3d virtual worlds," arXiv:1907.06007, 2019.
- [7] S. Long and C. Yao, "Unrealtext: Synthesizing realistic scene text images from the unreal world," arXiv:2003.10608, 2020.
- [8] Baek et al., "Character region awareness for text detection," in CVPR, June 2019.
- [9] Sun et al., "Chinese street view text: Large-scale chinese text reading with partially supervised learning," in ICCV, October 2019.
- [10] Qin et al., "Curved text detection in natural scene images with semi-and weakly-supervised learning," arXiv:1908.09990, 2019.
- [11] Zhang et al., "Uber-text: A large-scale dataset for optical character recognition from street-level imagery," in Scene Understanding Workshop-CVPR, 2017.
- [12] Epshtein *et al.*, "Detecting text in natural scenes with stroke width transform," in *CVPR*. IEEE, 2010, pp. 2963–2970.
- [13] L. Neumann and J. Matas, "A method for text localization and recognition in real-world images," in ACCV. Springer, 2010, pp. 770–783.
- [14] Jaderberg et al., "Reading text in the wild with convolutional neural networks," IJCV, vol. 116, no. 1, pp. 1–20, 2016.
- [15] Liao et al., "Mask textspotter: An end-to-end trainable neural network for spotting text with arbitrary shapes," IEEE t. PAMI, 2019.
- [16] Long *et al.*, "Textsnake: A flexible representation for detecting text of arbitrary shapes," in *ECCV*, 2018, pp. 20–36.
- [17] Jaderberg et al., "Spatial transformer networks," in NIPS, 2015, pp. 2017–2025.
- [18] K. Simonyan and A. Zisserman, "Very deep convolutional networks for large-scale image recognition," arXiv:1409.1556, 2014.
- [19] He et al., "Deep residual learning for image recognition," in CVPR, 2016, pp. 770–778.

- [20] Graves et al., "Connectionist temporal classification: labelling unsegmented sequence data with recurrent neural networks," in ICML, 2006.
- [21] Cheng *et al.*, "Focusing attention: Towards accurate text recognition in natural images," in *ICCV*, 2017, pp. 5076–5084.
- [22] Liu *et al.*, "Fots: Fast oriented text spotting with a unified network," in *CVPR*, June 2018.
- [23] Bušta et al., "E2e-mlt-an unconstrained end-to-end method for multilanguage scene text," in ACCV. Springer, 2018, pp. 127–143.
- [24] Qin *et al.*, "Towards unconstrained end-to-end text spotting," in *ICCV*, October 2019.
- [25] D.-H. Lee, "Pseudo-label: The simple and efficient semi-supervised learning method for deep neural networks," in Workshop on challenges in representation learning, ICML, vol. 3, 2013, p. 2.
- [26] Sun et al., "Chinese street view text: Large-scale chinese text reading with partially supervised learning," in ICCV, 2019, pp. 9086–9095.
- [27] Iwana et al., "Judging a book by its cover," arXiv:1610.09204, 2016.
- [28] Mishra et al., "Scene text recognition using higher order language priors," in BMVC, 2012.
- [29] Wang et al., "End-to-end scene text recognition," in ICCV. IEEE, 2011, pp. 1457–1464.
- [30] Trung *et al.*, "Recognizing text with perspective distortion in natural scenes," in *ICCV*, December 2013.
- [31] Lucas et al., "Icdar 2003 robust reading competitions," in ICDAR. Citeseer, 2003, pp. 682–687.
- [32] Karatzas et al., "Icdar 2013 robust reading competition," in ICDAR. IEEE, 2013, pp. 1484–1493.
  [33] Karatzas et al., "Icdar 2015 competition on robust reading," in ICDAR.
- 33] Karatzas et al., "Icdar 2015 competition on robust reading," in ICDAR. IEEE, 2015, pp. 1156–1160.
- [34] C. K. Chng *et al.*, "Total-text: Towards orientation robustness in scene text detection," *International Journal on Document Analysis and Recognition (IJDAR)*, vol. 23, pp. 31–52, 2020.
- [35] Risnumawan et al., "A robust arbitrary text detection system for natural scene images," Expert Systems with Applications, vol. 41, no. 18, pp. 8027–8048, 2014.
- [36] Baek et al., "What is wrong with scene text recognition model comparisons? dataset and model analysis," arXiv:1904.01906, 2019.
- [37] Liu *et al.*, "Star-net: A spatial attention residue network for scene text recognition." in *BMVC*, vol. 2, 2016, p. 7.
- [38] Shi et al., "Robust scene text recognition with automatic rectification," in CVPR, 2016, pp. 4168–4176.
- [39] Graves *et al.*, "Bidirectional lstm networks for improved phoneme classification and recognition," in *ICANN*, 2005, pp. 799–804.
- [40] S. Hochreiter and J. Schmidhuber, "Long short-term memory," *Neural computation*, vol. 9, no. 8, pp. 1735–1780, 1997.
- [41] Litman *et al.*, "Scatter: Selective context attentional scene text recognizer," *arXiv:2003.11288*, 2020.

[42] Lu et al., "Master: Multi-aspect non-local network for scene text recognition," arXiv:1910.02562, 2019.

# APPENDIX A BOUNDING BOX TRANSFORMATIONS

We define the following transformations to generate a set of bounding boxes in the neighbourhood of an input bounding box: Extending/shrinking the bounding box on the left/right/top. Angle modification and bottom extension/shrinkage were also considered but the benefits were insignificant. To keep the computational cost reasonable, we also assume that changes to the left side of the bounding box do not influence the recognition of the characters on the right side and vice versa, the optimization on each side is done independently. Horizontally, we extend/shrink the box with width w and height h in each direction by up to c characters, the character length being estimated as the average character length  $ch_{avg} = \frac{w}{|text|}$ . On the top, we extend by up to  $\frac{h}{\beta}$  and shrink by up to  $\frac{h}{\alpha}$ .

Each of the transformed bounding boxes can be characterized by three integer parameters relative to the original bounding box - (t,l,r) - defining the extension/shrink (distinguished by the sign) by t,l,r units on top/left/right, where the horizontal unit is  $\frac{ch_{avg}}{\delta}$  and the vertical unit is  $\frac{h}{\kappa}$ . Consequently,  $l,r\in[-c\cdot\delta;c\cdot\delta]$  and  $t\in[-\frac{\kappa}{\gamma};2\frac{\kappa}{\beta}]$ . The transformed bounding boxes that exceed the image or do not overlap with the original one are immediately discarded.

To obtain the final bounding box  $bb_f$  characterized by  $(t_f, l_f, r_f)$ , we find an optimal bounding box in both directions (left and right). For each direction, we find the set of boxes  $B = \{(t_i, l_i, r_i)\}_{i=1...n}$  that result in the lowest edit distance from g. The sets  $T = \bigcup_{(t_i, l_i, r_i) \in B} t_i$ ,  $L = \bigcup_{(t_i, l_i, r_i) \in B} l_i$  and  $R = \bigcup_{(t_i, l_i, r_i) \in B} r_i$  are created.

From the boxes transformed in the left direction, we obtain

$$t_l = \min T \tag{10}$$

and

$$l_f = \frac{\min L + \min(\max L, o + \min L)}{2} \tag{11}$$

Analogously, for the right direction, we obtain

$$t_r = \min T \tag{12}$$

and

$$r_f = \frac{\min R + \min(\max R, o + \min R)}{2} \tag{13}$$

We set

$$t_f = \max(t_r, t_l) \tag{14}$$

In our experiments, the constants were assigned as follows:  $c=7,\,\beta=2,\,\gamma=4,\,\delta=4,\,\kappa=4,\,o=8.$  They were selected by observing qualitative results, attempting to minimize the amount of incorrect PGTs without loosing too many of the correct ones. The optimal numbers may vary according to the E2E system used and a more elaborate parameter search will likely improve the results.

# APPENDIX B PGT ACCURACY

Different kind of errors can occur in the PGT, some more harmful than others. First, the different kind of errors we have encountered are listed and explained. We further report the error frequencies in Table VII, computed on 500 samples from the UT dataset and 500 samples from the ABC dataset.

In a lot of cases, it is not clear what should still be considered an error.

**Not text (I)** - the PGT image does not really contain any text - it was a false positive detection. Often, it is a very blurred image, or an image containing text-like patterns.

Wrong text (II) - the image does contain text but the PGT transcription is wrong - either just a small part, like a single character, or the whole text.

**Imprecise crop (III)** - either a part of a character from the next word is present in the image but not in the PGT transcription or a part of a character is missing.

**Unreadable** (**IV**) - the text in the image is unreadable for humans - either just a part of it or the whole text. Sometimes, context (language, scene) helps to determine the correct word.

**Punctuation** (V) - errors in punctuation, for example, a dot at the end of a word was not predicted.

**Weak label error (VI)** - there was an error in the weak label (typo, hyphenation, ...) which resulted in incorrect PGT. Type VI could be considered a subset of the type I error but type I errors are usually more serious as some datasets do not even contain punctuation.

Type I, II and VI errors are the most undesirable ones. However, employing some recognition confidence based filtering, type I and II are also the easiest ones to mitigate. This is because these errors mostly occur for some very blurred texts/images with no text, where the network predicts a short, common word such as the, in, on, at with low confidence.

The error classification is not always clear, some may overlap.

	ABC	UT	Examples
not text	1	2	the
wrong text	19	6	CONNER, cancer
imprecise crop	14	14	Java,
unreadable	5	20	the
punctuation	1	2	1:15 000 1:15,000
weak label error	0	7	hilling services

TABLE VII: The frequencies of different kind of errors on a subset of  $ABC_3$  and  $UT_6$  - 500 samples from each.